Bull Math Biol (2018) 80:1655–1687
https://doi.org/10.1007/s11538-018-0431-5

ORIGINAL ARTICLE

Plant Dynamics, Birth-Jump Processes, and Sharp Traveling Waves

N. Rodríguez[1] · **G. Malanson**[2]

Received: 10 July 2017 / Accepted: 6 April 2018 / Published online: 10 May 2018

Abstract Motivated by the importance of understanding the dynamics of the growth and dispersal of plants in various environments, we introduce and analyze a discrete agent-based model based on a *birth-jump process*, which exhibit wave-like solutions. To rigorously analyze these traveling wave phenomena, we derive the diffusion limit of the discrete model and prove the existence of traveling wave solutions (sharp and continuously differentiable) assuming a logarithmic-type growth. Furthermore, we provide a variational speed for the minimum speed of the waves and perform numerical experiments that confirm our results.

Keywords Birth-jump processes · Degenerate reaction–diffusion equation · Traveling wave solutions

1 Introduction

Global change has multiple components that are affecting the future existence of many species (Parmesan and Yohe 2003). The most widely recognized is climate change, but invasive species and land use change, often habitat destruction, are also important. All of these would seem to require the movement of organisms across landscapes in

✉ N. Rodríguez
nrod@unc.edu

G. Malanson
george-malanson@uiowa.edu

1 Department of Mathematics, UNC Chapel Hill, Phillips Hall, CB#3250, Chapel Hill, NC 27599-3250, USA

2 Department of Geographical and Sustainability Sciences, University of Iowa, Iowa City, IA 52242, USA

order to survive as species (i.e., through generations) (Travis et al. 2013). Thus, global change is driving ecological research with particular attention to spatial movement (Kot et al. 2004). A gap exists, however, between our ability to model the specifics of spatial movement in realistic landscapes (recognizing the difficulty of parameterizing even simplistic models), and the core theory of ecology. Whereas core theory is, by definition general and simple, it is expressed in mathematics that are the former but not the latter, and connection between theoretical models and applied models is piecemeal and incomplete.

We aim to improve the linkage of mathematical models of spatial ecological processes with the more specific models that are used in applications. At this stage, we take the step to develop processes in a simplified agent-based simulation based on established models in theoretical ecology. Agent-based models (ABMs) provide a simulation approach to the study of individuals interacting in an environment. ABMs descended from interacting particle systems via stochastic cellular automata and outside of computer science and engineering the agents are taken to represent individuals such as organisms existing in a spatially explicit environment, e.g., a grid of cells representing a landscape, and interacting with each other and the environment, e.g., reproducing only in some places. Agent-based modeling has been thoroughly reviewed from an ecological perspective (Grimm and Railsback 2005) and in other domains (Malanson and Walsh 2015). For our purpose, ABMs can simulate the reproduction, movement, and death of individuals on landscapes; the landscapes can vary in the effects of individual or multiple cells on these processes; the landscape can be complicated, with multiple attributes which are sometimes correlated and sometimes not. Furthermore, these processes can be influenced by other individuals, with or without distance dependence or other attributes. In their most extended form, ABMs have been used to examine the interactions of individuals responding to climate change across complicated landscapes (Dey et al. 2017; Redmond et Al. 2017) and in more abstract or stylized scenarios (Smith-McKenna et al. 2014; Mohd et al. 2016). ABMs, while designed to be specific, can be general. They can approximate the simplicity of more elegant mathematical models, but only through sacrificing their strengths and even then, in addition to being inelegant, cannot easily be further analyzed through reference to established mathematical principles.

In Malanson and Rodríguez (2017), we use simulations to produce an analysis typical of theoretical ecology. It is the purpose of this paper to extend the work in Malanson and Rodríguez (2017) and perform an analyses that cannot be done simply through the use of ABMs. This step sets the stage for further work in which the more mathematically based and the more simulation-based approach can develop a dialectic to advance how we understand the behavior of ecological systems and how we anticipate specific consequences of global change. For this purpose, we derive a continuous model from the ABM for plant dynamics that is more amenable for analysis. The outcomes are a family of nonlinear-degenerate integro-differential equations arising from a *birth-jump* process (Hillen et al. 2015). A *birth-jump* integro-differential equation describes a population or trait for which dispersal cannot be decoupled from birth. These types of models were introduced recently (see Hillen et al. 2015) as a generalization to integro-differential equations that arise from a *position-jump process* (a stochastic process that generalizes random walks (Murray 2004; Hutson and Martinez

2003; Othmer et al. 1988) in that individuals are allowed to make spatial jumps with a given probability) or reaction–diffusion equations (Cantrell et al. 2003).

For some cases we see that the equation can be degenerate with the degeneracy arising when the density is zero. This would model, for example, the idea that in some cases the probability that a plant can produce a seed degenerates to zero as the density of plants in a region goes to zero. The idea referred to as the positive feedback switch (Wilson and Agnew 1992) is that in high stress environments individuals can alter the environment to favor neighbors of their own kind. For example, at alpine treeline a tree reduces wind speed, which means less evapotranspirative stress, more deposition of new sediment, more snow (which sometimes is the important source of water), reduced night cooling, and possible UV damage: all of which favor new tree seedlings over already established alpine tundra species (Malanson et al. 2011). The sharp boundaries sometimes seen at treelines might then be linked to zero density and sharp traveling waves. Sharp waves would in turn imply a specific relationship between a spatial pattern, feedback, and potential rate of advance of one type of vegetation into another, and these might be part of a range of such relations (e.g., Zeng and Malanson 2006). Observation and modeling of traveling waves of expanding patterns of bacteria in Petri dishes have considered sharp waves (e.g., Kawasaki et al. 1997; Satnoianu et al. 2001; Mansour 2007; Jalbert and Eberl 2014), but sharp waves have not been modeled for jump-dispersal processes to the best of our knowledge.

In this work we aim to derive a continuum model form the ABM model and compare the results numerically and to analyze the continuum model in a more rigorous fashion that is not afforded by the ABM. In the diffusion limit we prove the existence of traveling wave solutions when the reaction term in the continuum model is of monostable type (e.g., Yagisita 2009; Coville and Dupaigne 2007; Li et al. 2010). Furthermore, in this same limit we obtain a degenerate reaction–diffusion equation, for which "sharp traveling waves" (Sánchez-Garduño and Maini 1995) exist for certain proliferation, establishment, and mortality rate functions. We explore the existence and uniqueness of such traveling waves under a variety of circumstances and prove the existence of a minimum speed for which such traveling waves exist. The method used here is based on those developed in Sánchez-Garduño and Maini (1994), Sánchez-Garduño and Maini (1995).

2 Agent-Based Model

2.1 Overview

We summarize the ABM of the process described in Malanson and Rodríguez (2017). We represent the habitat as the two-dimensional Euclidean space $\mathbb{R}^2$ that we discretize into a lattice with $\mathbf{x}_{ij} = (x_i, y_j)$ representing the nodes. For simplicity, assume that both the x-axis and y-axis discretizations are of size ℓ. That is, $\mathbf{x}_{ij} = (i\ell, j\ell)$ with $i, j \in \{0, \pm 1, \pm 2, \ldots, \pm n, \ldots\}$. We also discretize time into periods of δt time. Since the growth and the spread of plants cannot be decoupled we use a *birth-jump process* (see Hillen et al. 2015) to model the dynamics of plant dispersal and growth. The core process that we examine has been called birth jump because the subpro-

cesses of reproduction and dispersal are inextricably linked. This process, however, is the same as represented in many ecological models as the stages of reproduction and dispersal—when the latter is "jump dispersal" [sensu Pielou (1977) but without environmental heterogeneity a prerequisite], not contagious diffusion. The process consists of the reproduction of a new individual by a parent and the immediate dispersal of the new individual. The parent may or may not die after a single reproduction (semelparous vs. iteroparous reproduction as in annual vs. perennial plants). Unlike with some animals, dispersal is in the same time step as reproduction. As noted above, the dispersal step is critical and the advance of a species into new territory will depend on its dispersal kernel. The shape of kernels has been studied extensively, and the central finding for patterns of invasion and response to climate change for plant species is that a fat-tailed kernel, i.e., not exponentially bounded, would be necessary in a model for it to match observations. Some examples include the spread of species northwards after the retreat of ice sheets from the Last Glacial Maximum. As mentioned earlier birth-jump processes are generalization of *position-jump processes*. Note here that since plants do not move there are no position-jump processes in these dynamics.

For the purpose of describing the ABM dynamics let $n_{ij}(t)$ be the number of plants located at location $\mathbf{x}_{ij}$ and time t. Let us consider how the number of plants changes from time t to time $t + \delta t$, with $\delta t > 0$ given. At location $\mathbf{x}_{ij}$ we have that:

$$\begin{aligned}\#\text{ of plants at time } t + \delta t = &\text{ arriving seeds that germinate}\\ &+ \text{surviving plants from time } t.\end{aligned}$$

The first term on the right-hand-side (RHS from here on) is the *proliferation* term, which accounts for the production of seeds that end in location $\mathbf{x}_{ij}$ germinate. Let $p_\beta(\mathbf{y})$ be probability that a plant at location $\mathbf{y}$ will produce a seed during the period $(t, t + \delta t)$. This can depend on the favorability of the environment as well as on the number of plants at that location. Let $s_{\mathbf{xy}}$ be the *relocation probabilities*: the probability that a seed from a plant at location $\mathbf{y}$ will land in location $\mathbf{x}$. Then, the total proliferation term in location $\mathbf{x}_{ij}$ is given by:

$$\sum_{k=-\infty}^{\infty}\sum_{m=-\infty}^{\infty} p_\beta(\mathbf{x}_{km}) s_{\mathbf{x}_{km}\mathbf{x}_{ij}} n_{km}(t).$$

Naturally, the probability that a seed actually germinates in location $\mathbf{x}_{ij}$ can be a function of the density of plants at that location (possibly taking into account the volume-filling effect or the positive feedback switch) and of the environmental conditions there. Let $p_g(\mathbf{x})$ be the probability that a seed at location $\mathbf{x}$ will germinate. We assume that germination happens immediately; however, in reality there is a time delay, but we defer the derivation of a model that includes this effect for future work. Taking the above assumptions into account, a more realistic proliferation term is given by:

$$\sum_{k=-\infty}^{\infty}\sum_{m=-\infty}^{\infty} p_\beta(\mathbf{x}_{km}) p_g(\mathbf{x}_{ij}) s_{\mathbf{x}_{km}\mathbf{x}_{ij}} n_{km}(t).$$

Finally, consider the *survival* term, which can also depend on the environment and/or the number of plants at the location. Consider this term as:

$$(1 - p_\delta)n_{ij}(t),$$

where p_δ is the probability that a plant will die (stop reproducing and open up space for other plants to grow) at that location during the period $(t, t + \delta t)$. Combining the above assumptions we obtain the discrete equation:

$$n_{ij}(t + \delta t) - n_{ij}(t) = \sum_{k=-\infty}^{\infty} \sum_{m=-\infty}^{\infty} p_\beta(\mathbf{x}_{km}) p_g(\mathbf{x}_{ij}) s_{\mathbf{x}_{km}\mathbf{x}_{ij}} n_{km}(t) - p_\delta(\mathbf{x}_{ij}) n_{ij}(t). \tag{1}$$

2.1.1 Proliferation and Germination Probabilities

In this section, we discuss possible proliferation, germination, and survival probabilities. For a specific example, consider the case when the number of seeds that one plant produces a seed is a Poisson process with expected number seeds either dependent or independent on the number of plants. If the probability of a plant producing a seed is independent of number of plants in the immediate neighborhood, then it is reasonable to assume that the expected number of seeds produced by a plant at location $\mathbf{x}_{ij}$ during the time period $(t, t + \delta t)$ is given by $\tilde{\beta}\delta t$ where $\tilde{\beta} \geq 0$ is a constant rate with units seeds/(plant $\times$ T) with T representing the time units. Inclusion of the environment would lead to $\tilde{\beta}(\mathbf{x}_{ij})$. Hence, the probability that a plant will generate a seed during this time is given by:

$$p_\beta = 1 - \mathrm{e}^{-\tilde{\beta}(\mathbf{x}_{ij})\delta t}.$$

If the number of seeds produced by any one plant at location $\mathbf{x}_{ij}$ is dependent on the number of plants we have instead that:

$$p_\beta(\mathbf{x}_{ij}) = 1 - \mathrm{e}^{-\tilde{\beta}(\mathbf{x}_{ij}, n_{ij})\delta t}.$$

Similarly, assume that the expected number of seeds that germinate into a plant during the period $(t, t + \delta t)$ is given by $\tilde{g}\delta t$. Hence, we have that

$$p_g(\mathbf{x}_{ij}) = 1 - \mathrm{e}^{-\tilde{g}(\mathbf{x}_{ij})\delta t},$$

where g has units of plants/(seeds $\times$ T). Finally, assume that

$$p_\delta(\mathbf{x}_{ij}) = 1 - \mathrm{e}^{-\delta(\mathbf{x}_{ij})\delta t}.$$

Note that adding density dependence on the germination and the death probabilities is done similarly to that of the proliferation probability.

2.2 Simulation Algorithm and Results

We report traveling wave solutions for our ABM (Malanson and Rodríguez 2017). This ABM simulated the birth-jump process plus establishment for no-tail, thin-tail, and fat-tail dispersal kernels (random uniform, Gaussian, and Cauchy kernels, respectively). Probabilities were based on either population density or habitat, and for the latter as homogeneous or on a gradient, and if a gradient is considered we added positive feedback from populations to the habitat; these comprise 12 scenarios. The uniform and Gaussian kernels produced traveling waves with constant speed, but the fat-tailed Cauchy kernel produced traveling waves that accelerated and also flattened as the low-probability portion of wave accelerated fastest. A greater variety of spatial patterns were able to develop among the replicate simulations of the fat-tailed kernel (Fig. 1).

3 Continuous Model

3.1 Derivation

In this section we derive the continuum limit from the ABM model [see Hillen et al. (2015) for a similar derivation without germination in one dimension]. To accomplish this, take the limit as δx and δt go to zero, moving from having a discrete number of plants to a density of plants with the relationship:

$$u(\mathbf{x}, t) = n_{ij}/\ell^2.$$

One can think of $u(\mathbf{x}, t)$ as giving the probability that there is a plant at location x and time t. After minor algebraic manipulations of (1) we obtain the equation for the density as

$$\frac{u(\mathbf{x}, t+\delta t) - u(\mathbf{x}, t)}{\delta t} = \frac{1}{\delta t} \sum_{k=-\infty}^{\infty} \sum_{m=-\infty}^{\infty} p_\beta(\mathbf{x}_{km}) p_g(\mathbf{x}_{ij}) s_{\mathbf{x}_{ij}\mathbf{x}_{ij}} u(\mathbf{y}_{km}, t) - \frac{1}{\delta t} p_\delta(\mathbf{x}_{ij}) u(\mathbf{x}, t).$$

In the above equation we assume that the probabilities are independent of the densities (a similar computation follows if the probabilities are density-dependent). A Taylor series expansion for $p_\beta(\mathbf{x}_{km}) p_g(\mathbf{x}_{ij})$ and p_δ then yields:

$$p_\beta(\mathbf{x}_{km}) p_g(\mathbf{x}_{ij}) = \tilde{\beta}\tilde{g}\delta t^2 + O(\delta t^3) \quad \text{and} \quad p_\delta = \delta\delta t + O(\delta t^2).$$

Finally, we define the continuous redistribution potential as $S(\mathbf{x}, \mathbf{y}) = s_{ij}/\ell^2$; thus, we rewrite (1) in the continuous variables:

$$\frac{u(\mathbf{x}, t+\delta t) - u(\mathbf{x}, t)}{\delta t} = \sum_{k,m=-\infty}^{\infty} S(x, \mathbf{y}_{km}) \tilde{\beta}(u(\mathbf{y}_{km}, t), y) \tilde{g}(u(x, t), x) u(\mathbf{y}_{km}, t) \ell^2 \delta t$$

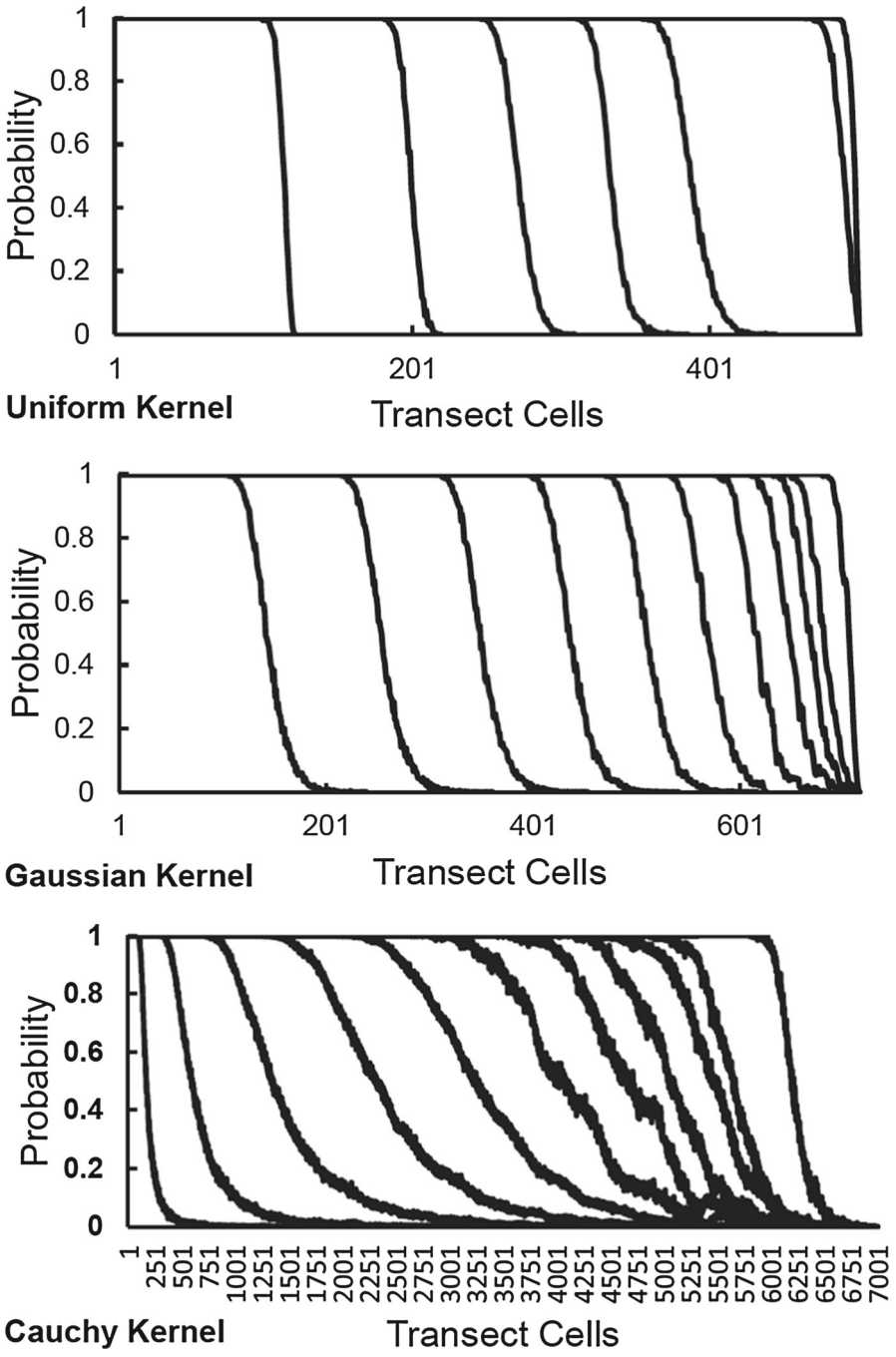

Fig. 1 Traveling waves at 100, 200, 300, 400, 500, 1000, and 1500 iterations for the three kernels used in the ABM simulations with an environmental gradient in which the habitat quality decreases from 1–0 over the length of the transect at a rate such that the advancing wave reaches 0.5 at 500 iterations

$$- \delta(u(\mathbf{x}, t), \mathbf{x})u(\mathbf{x}, t) + O(\delta t).$$

Taking the limit as $\delta t, \ell^2 \to \infty$ such that $\beta g = \tilde{\beta}\tilde{g}\delta t$ remains constant we recognize the first term on the right-hand-side as a Riemann sum and obtain:

$$u_t(x, t) = \int_{\mathbb{R}^2} S(x, y)\beta(u(y, t), y)g(u(x, t), x)u(y, t)\, \mathrm{d}y - \delta(u(x, t), x)u(x, t),$$

where we drop the bold notation for simplicity (that is we go from $\mathbf{x} \to x$).

3.1.1 Redistribution Potential

For plant dynamics we see that seeds mainly disperse via gravitational, wind, and animal transport methods (Horvitz et al. 2015). Note that in our model each particular seed can only be dispersed via one of these methods, although combinations exist in nature. Let p_1 be the probability that a seed disperses via gravity (falls close to the mother plant with high probability); p_2 be the probability that the seed is transported via wind; and p_3 the probability that a seed is consumed by an animal (to be deposited somewhere else later). Thus, we assume that $\sum_{k=1}^{3} p_k = 1$. To fully account for these different modes of transportation we must consider three different redistribution potential: one that models the redistribution due to gravity S_1, one that models redistribution due to the wind S_2, and one that models redistribution due to animals S_3. Hence, under these assumptions we have that

$$\begin{aligned} u_t(x, t) = &\sum_{n=1}^{3} p_n \int_{\mathbb{R}} S_n(x, y)\beta(u(y, t), y)g(u(x, t), x)u(y, t)\, \mathrm{d}y \\ &- \delta(u(x, t), x)u(x, t). \end{aligned} \tag{2}$$

For example, a reasonable assumption for the gravity potential is that it is radially symmetric, decreasing and rapidly decaying. The Gaussian potential is a very reasonable probability function to use here and the potential due to wind could be unidirectional, accounting for the direction of the wind. The potential due to animal redistribution can be a characteristic function such as $\frac{1}{2a}\chi_{[-a,a]}(x)$ indicating a uniform distribution over the interval $[-a, a]$ for some $a > 0$.

3.1.2 Diffusion Limits

We approximate the non-local Eq. (2) with a local version using moment approximations. Much effort has gone into analyzing fully non-local models where the non-local term arises from position-jump processes. Traveling wave solutions are known to exist for such models with reaction terms of bistable, monostable, and ignition type. Ermentrout and McLeod obtained the first results in Ermentrout and McLeod (1993) where they proved the existence and uniqueness of traveling wave solutions for a non-local neural network. Four years later, Bates, Fife, Ren, and Wang obtained results for a more general equation in Bates et al. (1997). Chen (1997), Coville (2007), and

Coville and Dupaigne (2007) have made significant contributions to the theory since then. However, the analysis of models where the non-locality arises from birth-jump processes is more involved and to the authors' knowledge no such theory has been developed. Hence, to be able to push the theory a step forward we look at the diffusion limit in one dimension noting that an extension to two-dimensions is trivial. Namely, we are concerned about approximating the terms:

$$\int_{\mathbb{R}} S_i(x, y)\beta(u(y,t), y)g(u(x,t), x)u(y,t)\,\mathrm{d}y$$

for $i = 1, 2, 3$. For this purpose let $h(y,t) = \beta(u(y,t), y)u(y,t)$ and assume that β is regular enough to allow for a Taylor series expansion of h about $y = x$:

$$\begin{aligned}\int_{\mathbb{R}} S_i(x, y)h(y,t)g(u(x,t))\mathrm{d}y &= \int_{\mathbb{R}} S_i(x, y)g(u(x,t), x)\sum_{k=0}^{\infty}\frac{1}{k!}\partial_x^k h(x,t)(y-x)^k\mathrm{d}y \\ &= g(u(x,t), x)\sum_{k=0}^{\infty} M_k^i(x)\partial_x^k h(x,t) \\ &= g(u(x,t), x)\sum_{k=0}^{\infty} M_k^i(x)\partial_x^k[\beta(u(x,t), x)u(x,t)],\end{aligned}$$

where

$$M_k^i(x) = \frac{1}{k!}\int_{\mathbb{R}} S_i(x, y)(y-x)^k\,\mathrm{d}y$$

are the kth moments of S_i. Thus, if the moments exist and form an asymptotic sequence one can safely truncate after the first few moments.

Symmetric potentials with finite second moment Considering a second-moment approximation with symmetric potentials gives:

$$\begin{aligned}u_t(x,t) = &\sum_{n=1}^{3} p_n M_2^n(x)g(u(x,t), x)\partial_{xx}(\beta(u(x,t), x)u(x,t)) \\ &+\left(\sum_{n=1}^{3} p_n M_0^n(x)g(u(x,t), x)\beta(u(x,t), x) - \delta(u(x,t), x)\right)u(x,t).\end{aligned} \tag{3}$$

If the potentials have finite second moments and the habitat is spatially homogeneous then (3) simplifies to

$$u_t = dg(u)(\beta(u)u(x,t))_{xx} + (g(u)\beta(u) - \delta(u))u(x,t), \tag{4}$$

where $d = \sum_{n=1}^{3} s_n M_2^n$ and $\sum_{n=1}^{3} s_n M_0^n = 1$.

Anisotropic potentials are important in application and have been used to model collective behavior in biological aggregation (Evers et al. 2014; Brecht and Uminsky 2017). Moreover, traveling wave solutions have also been studied for non-local reaction–diffusion equations with asymmetric potentials, see for example Coville et al. (2008), Sun et al. (2011). While a derivation for asymmetric potentials is more complicated it can be done for special cases. However, we leave the derivation of this limiting process for future work.

4 Traveling Wave Solutions

One important issue of interest to ecologist is the ability of a species to invade new habitats and of forest declines (Ruckstuhl et al. 2008; Betts et al. 2004). These are of particular interest since they are heavily related to two of the nine "tipping points in climate change" (Schellnhuber 2009). To attempt to understand these issues from a theoretical perspective one is prompted to look for *traveling wave solutions*. In this section we explore and analyze the existence of such waves for various reaction terms. Moreover, in the case when (4) describes the positive feedback switch, leading to a degenerate reaction–diffusion equation we prove the existence of **sharp waves**—see Definition 2. Figure 3 illustrates such waves. To move forward with our analysis we rewrite Eq. (4) as follows:

$$\frac{1}{g(u)}u_t = (D(u)u_x)_x + f(u), \tag{5}$$

where

$$D(u) := \beta'(u)u + \beta(u) \quad \text{and} \quad f(u) := \left(\beta(u) - \frac{\delta(u)}{g(u)}\right)u.$$

The traveling wave solution $U(z)$, a function of the moving coordinate $z = x - ct$, which we seek satisfies:

$$D(U)U'' + D'(U)(U')^2 + f(U) + \frac{c}{g(U)}U' = 0, \tag{6}$$

along with suitable conditions at $\pm\infty$. The existence and qualitative properties of traveling wave solutions to (5) are known to be tied to the reaction term $f(u)$. In fact, in the case when $D(u)$ and $g(u)$ are positive constants, Eq. (5) reduces to the well-analyzed reaction–diffusion equation (Britton 1986). In that case there are three typical types of reaction terms which have been studied: *monostable* where f has two critical points and represents growth up to a carrying capacity; *bistable* where f has three critical points and represents growth above some positive threshold and up to a carrying capacity; *ignition type* where $f(u) = 0$ for $u \in [0, \theta)$ and positive up to a carrying capacity (for some $\theta > 0$).

For the remainder of this work assume that $f(u)$ is of monostable type:

$$f(0) = f(1) = 0,\ f(z) > 0 \text{ for } z \in (0, 1) \text{ and } f < 0 \text{ otherwise.} \tag{7}$$

Moreover, assume that:

$$f(z)D(z) \leq f'(0)D(0)z \quad \text{for} \quad z \in (0,1), \tag{8}$$

and

$$\lim_{z\to 1} \frac{f(z)}{1-z} < \infty, \tag{9}$$

i.e., f approaches zero faster or at the same rate that z approaches one. Condition (8) is the so-called *linear determinacy* (Hillen et al. 2015).

4.1 Continuously Differentiable Traveling Wave Solutions

First, consider the case of *continuously differentiable traveling waves*. For a concrete example take the following functions:

$$g(u) = \frac{1}{1+u}, \ \beta(u) = \mu(\gamma + u), \ \delta(u) = \mu u, \tag{10}$$

with $\mu, \gamma > 0$. In this case Eq. (6) is a uniformly parabolic equation since $D(u) \geq \mu\gamma$ for all $u \geq 0$ and classical theory for parabolic equations can be applied here. For the functions given by (10) we observe the existence of a continuously differentiable traveling wave solution to (5), which is illustrated in Fig. 2.

Definition 1 (*Continuously differentiable traveling waves*) A *smooth traveling wave solution* of (5) is a continuously differentiable function $U(z)$ satisfying (6) with

$$U(-\infty) = 1 \quad \text{and} \quad U(+\infty) = 0,$$

and $0 < U < 1$ for all $z \in \mathbb{R}$.

In order to develop a more general theory, in this section we make the assumptions for $r \geq 2$:

(H1) $D \in C^r([0,\infty))$, $D(z) > 0$ for $z \in [0,1]$.
(H2) $g \in C^r([0,\infty))$, $g(z) > 0$ and $g'(z) < 0$ for $z \in [0,1]$.
(H3) $f \in C^r([0,\infty))$, $f'(1) < 0$.

Let $V = D(U)U'$ then (5) can be written as a system of two ODEs:

$$\begin{cases} U' = \frac{V}{D(U)}, \\ V' = -\frac{cV}{g(U)D(U)} - f(U). \end{cases} \tag{11}$$

The functions of the RHS of (11) are locally linear functions as $D, g > 0$ and continuously differentiable; hence, we have hopes of applying the Hartman Grobman

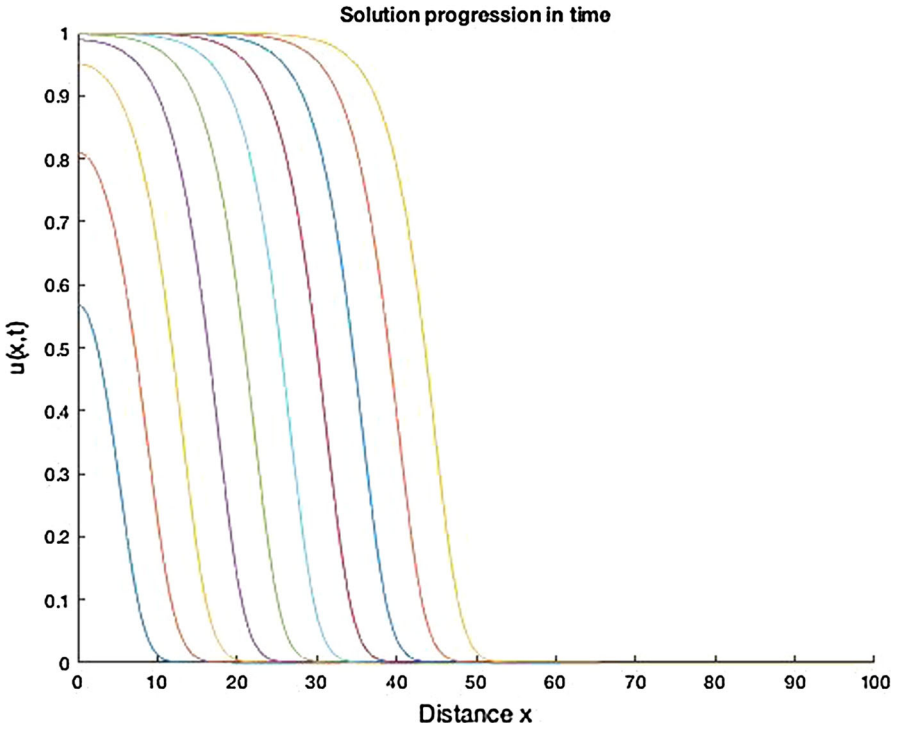

Fig. 2 (Color figure online) Continuously differentiable traveling wave for functions given by (10)

Theorem. Indeed, a simple linear analysis of (11) about the steady state $(0, 0)$ gives that in the case that $f'(0) > 0$ the steady state $(0, 0)$ is a saddle point provided

$$c \geq 2g(0)\sqrt{f'(0)D(0)}.$$

This gives the *minimum speed* for which traveling waves can exist:

$$c^* = 2g(0)\sqrt{f'(0)D(0)}. \tag{12}$$

Note that this reduces to the minimal speed for the case when $g \equiv 1$ obtained in the work of Hillen et al. in Hillen et al. (2015). Moreover, it can be seen that the point $(1, 0)$ is always a saddle point with eigenvalues given by

$$r_{\pm} = -\frac{c}{2g(1)D(1)} \pm \frac{1}{2}\sqrt{\left(\frac{c}{g(1)D(1)}\right)^2 - \frac{4f'(1)}{D(1)}}.$$

Recall that $f'(1) < 0$ and thus $r_+ > 0$. The eigenvector associated to the unstable direction is given by $\left(\frac{1}{D(1)}, r_+\right)$ and thus lies on the second and fourth quadrant. In essence, the traveling wave solutions we seek are heteroclinic connections leaving

$(1, 0)$ from the unstable direction and arriving at $(0, 0)$. Our first main result states that such heteroclinic connection exists for $c \geq c^*$.

Theorem 1 *Assume that (H1–H3) hold and that f satisfies (7)–(9). Then, there exists a traveling wave solution for all $c \geq c^*$ and no traveling wave solution exists for $c < c^*$.*

The proof is standard and consists of finding a region that traps the trajectory leaving the steady state $(1, 0)$ in the unstable direction.

Proof (Existence) Let $c \geq c^*$ and define the triangle T enclosed by the lines $\ell_1 := \{V = 0\}$, $\ell_2 := \{V = -\gamma U\}$ and $\ell_3 := \{V = -\alpha(1 - U)\}$ for some $\alpha, \gamma > 0$ to be determined later. Note that on ℓ_1 we have $U' = 0$ and $V' < 0$ and so the trajectories on that boundary ∂T point inwards. Next, for ℓ_2 we have that $U' < 0$ and

$$\frac{\mathrm{d}V}{\mathrm{d}U} = -\frac{c}{g(U)} + \frac{f(U)D(U)}{\gamma U}.$$

Notice that for the trajectories on this boundary to point toward T we need $\mathrm{d}V/\mathrm{d}U < -\gamma$ or equivalently if:

$$\frac{f(U)D(U)}{U} \leq -\gamma^2 + \frac{c\gamma}{g(U)}.$$

Now, using assumptions (H1)–(H2) and (8) we observe that the above inequality holds if:

$$\gamma^2 - \frac{c\gamma}{g(0)} + f'(0)D(0) \leq 0,$$

which holds for some values of γ if and only if $c \geq c^*$. Finally, we check that on ℓ_3 the trajectories also point toward T. On this boundary, we have that $U' < 0$ and that:

$$\frac{\mathrm{d}V}{\mathrm{d}U} = -\frac{c}{g(U)} + \frac{f(U)D(U)}{\alpha(1 - U)},$$

and know that the trajectories point inward toward T provided $\mathrm{d}V/\mathrm{d}U < \alpha$ or equivalently if:

$$\frac{f(U)D(U)}{(1 - U)} < \alpha^2 + \frac{c}{g(0)}\alpha,$$

which holds for α sufficiently large since the LHS remains bounded due to (9). As the trajectory leaving $(1, 0)$ along the unstable direction must remain inside T and there are not other fixed points it T it must approach $(0, 0)$. This gives the heteroclinic orbit we seek.

(Nonexistence) For $c < c^*$ the local analysis above proves that no trajectory leaving from $(1, 0)$ can approach $(0, 0)$. □

4.2 Sharp Traveling Wave Solutions

In this section, we consider the case when β depends only on the density itself. We observe that, in some cases, this can lead to degenerate equations that have traveling waves with a sharp transition. For example, consider the functions:

$$g(u) = \frac{1}{1+u}, \ \beta(u) = \mu u, \ \delta(u) = \bar{\mu} u, \tag{13}$$

with $0 < \bar{\mu} < \mu$. This implies that

$$f(u) = u^2[\mu - \bar{\mu} - \bar{\mu} u] \quad \text{and} \quad D(u) = 2\mu u, \tag{14}$$

in order to maintain a logarithmic-type growth. These functions generate the so-called *sharp traveling waves*—refer to Definition 2. Observe that f given in (14) does not satisfy (7) as it is positive for $z < 0$. This term is actually a degenerate bistable term, which is more subtle to treat. Here, we only provide a local nonlinear analysis in this case.

The degeneracy of $D(u)$, *i.e.,* $D(0) = 0$, in the above example leads (5) to become an ODE when $u = 0$ and a parabolic PDE for $u > 0$. It is this property that leads to the *sharp traveling waves* (see Sánchez-Garduño and Maini 1994, 1995), which are illustrated in Fig. 3. We provide a precise definition below for these types of waves.

Definition 2 (*Sharp traveling wave*) If there exists a value c and $z^* \in \mathbb{R}$ such that $U(x - ct)$ satisfies (6) for all $z \in (-\infty, z^*)$ and

$$\begin{aligned} &U(-\infty) = 1, \quad U(z^{*-}) = U(z^{*+}) = 0, \quad \text{and} \quad U(z) = 0 \text{ for } z \in (z^*, \infty); \\ &U'(z^{*-}) = -\frac{c}{g(0)D'(0)}, \quad U'(z^{*+}) = 0, \quad U'(z) < 0 \text{ for } z \in (z^*, \infty), \end{aligned} \tag{15}$$

then $U(x - ct)$ is a traveling wave solution with speed c of the **sharp-type**.

In spite of the degeneracy, for such traveling wave solutions we can still determine a variational formula for the speed.

Proposition 1 *A sharp traveling wave solution $U(x - ct)$ of (6) [in the sense of Definition (2)] has speed c satisfying the following variational formula:*

$$c = \frac{\int_0^{U(-\infty)} D(w)h(w)\mathrm{d}w}{\int_{-\infty}^{z^*} \frac{D(U)}{g(U)}(U')^2 \, \mathrm{d}z}. \tag{16}$$

Proof Multiply (6) by $D(U)U'$ and integrate on $(-\infty, z^*)$

$$\int_{-\infty}^{z^*} D^2(U)U''U' + D(U)D'(U)(U')^3 + D(U)f(U)U' + c\frac{D(U)}{g(U)}(U')^2 \, \mathrm{d}z = 0,$$

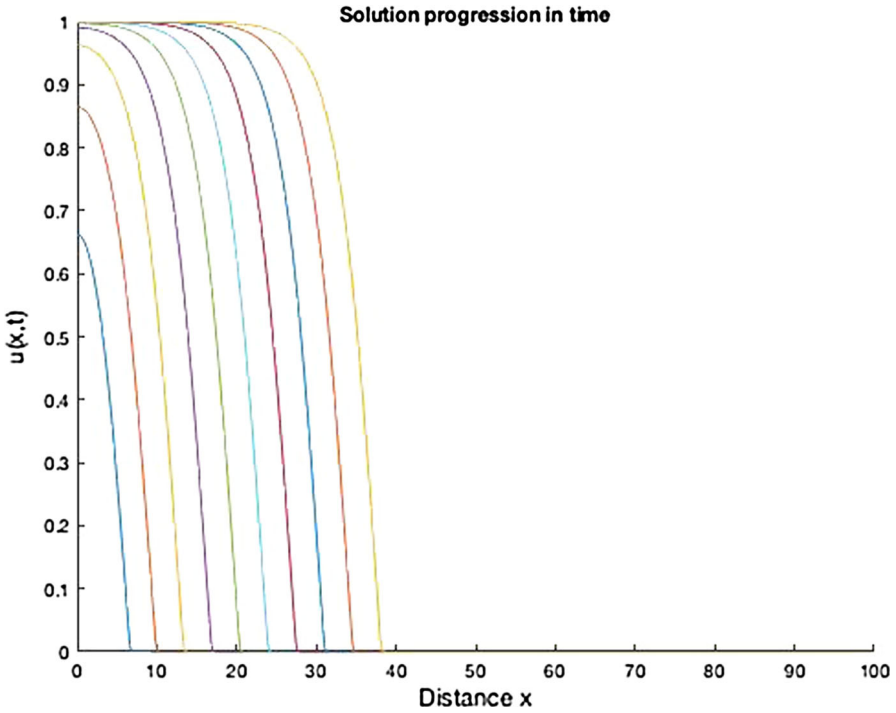

Fig. 3 (Color figure online) Sharp traveling wave

which is equivalent to:

$$\frac{\mathrm{d}}{\mathrm{d}z}\int_{-\infty}^{z^*}\frac{1}{2}\left[(D(U)U')^2\right]-\int_0^{U(-\infty)}D(w)f(w)\mathrm{d}w+c\int_{-\infty}^{z^*}\frac{D(U)}{g(U)}(U')^2\,\mathrm{d}z=0.$$

Now, given that

$$\begin{aligned}\frac{\mathrm{d}}{\mathrm{d}z}\int_{-\infty}^{z^*}\frac{1}{2}\left[(D(U)U')^2\right]&=\frac{1}{2}\left[(D(U(z^*))U'(z^*))^2-(D(U(-\infty))U'(-\infty))^2\right]\\&=0.\end{aligned}$$

From the above computations we obtain that c satisfies (16). □

Remark 1 From (16) one can observe that the volume-filling effect (represented by g) reduces the speed of the wave.

4.2.1 Main Results for the Degenerate Case

In this subsection, we state and prove our main result for the case when $D(u)$ degenerates at zero. The proof relies on techniques developed in Sánchez-Garduño and Maini

(1994), Sánchez-Garduño and Maini (1995) where they consider the $g \equiv 1$ case. With this objective in mind, assume the following conditions on the diffusion:

(A1) $D(0) = 0,\ D(u) >, D'(U) > 0$ and $D''(U) \neq 0$.

In addition, for the local nonlinear analysis we consider two different sub-cases for the function f, which differentiate between a monostable given when (M) holds and a degenerate bistable case when (DB) is satisfied:

(M) $f'(0) \neq 0$;
(DB) $f'(0) = 0,\ f''(0) > 0$.

We prove the following result in the case that f satisfies (M).

Theorem 2 (Existence and sharp traveling waves) *Let D, f and g satisfy $(A1)$, $(H2)$, $(H3)$, (7)–(9). There exists a c^* such that Eq. (5):*

(i) *has no traveling wave solutions for speed $c < c^*$.*
(ii) *has a traveling wave solution $U(x - c^*t)$ of the sharp-type satisfying (15).*
(iii) *for $c > c^*$ has a strictly monotone continuously differentiable traveling wave solution $U(x - ct)$ satisfying $U(-\infty) = 1$ and $U(+\infty) = 0$.*

The following analysis will set the stage for the proof of Theorem 2.

4.2.2 Nonlinear Local Analysis

As mentioned earlier, a traveling wave solution connecting the unstable zero steady state to a stable positive steady state is nothing more than a heteroclinic connection between these two steady states in the phase plane. To explore the possibility that such a connection exists, we rewrite (6) as a system of ODEs. For this purpose, let $V = U'$ then we have:

$$\begin{cases} U' = V, \\ D(U)V' = -D'(U)V^2 - f(U) - \frac{c}{g(U)}V. \end{cases} \tag{17}$$

Note that (17) has a singularity at $U = 0$ due to assumption (A1). To remove this singularity we perform the change of variables:

$$\tau = \int_0^z \frac{\mathrm{d}s}{D(u(s))} \Rightarrow \frac{\mathrm{d}\tau}{\mathrm{d}z} = \frac{1}{D(u(z))},$$

which is well-defined except maybe at the origin. Under this change of variables (17) becomes

$$\begin{cases} U' = D(U)V, \\ V' = -D'(U)V^2 - f(U) - \frac{c}{g(U)}V. \end{cases} \tag{18}$$

Observe that (18) has three steady states $P_0 := (0, 0), P_1 := (1, 0), P_c := \left(0, -\frac{c}{g(0)D'(0)}\right)$. Note that P_c depends on the speed c and that there is a saddle-node bifurcation for $c = 0$ when $P_0 = P_c$ leaving us with only two steady states in

that case. We begin with a nonlinear local analysis of the equation of interest in the case when (M) is satisfied.

Case 1: Monostable case $f'(0) \neq 0$: First, we study the stability of these steady states. Let $F(U,V) := D(U)V$ and $G(U,V) := -D'(U)V^2 - f(U) - \frac{c}{g(U)}V$, the Jacobian matrix is given by

$$J[F,G]_{(U,V)} = \begin{bmatrix} D'(U)V & D(U) \\ \frac{cVg'(U)}{[g(U)]^2} - f'(U) - D''(U)V^2 & -\frac{c}{g(U)} - 2D'(U)V \end{bmatrix}. \tag{19}$$

Hence, at P_0 we have:

$$J[F,G]_{(0,0)} = \begin{bmatrix} 0 & 0 \\ -f'(0) & -\frac{c}{g(0)} \end{bmatrix}, \tag{20}$$

which has eigenvalues $\lambda_1 = 0$ and $\lambda_2 = -\frac{c}{g(0)} < 0$, with respective eigenvectors $(c/g(0), -f'(0))^{\mathrm{T}}$ and $(0,1)^{\mathrm{T}}$. Hence, we conclude that P_0 is a non-hyperbolic equilibrium, and thus, it is insufficient to study the linearization of (18). To understand the behavior of the system near this equilibrium we need a second-order approximation of that system. This is given by:

$$\begin{cases} U' = D'(0)UV, \\ V' = -f'(0)U - \frac{cV}{g(0)} + G_2(U,V), \end{cases} \tag{21}$$

with

$$G_2(U,V) := -\frac{f''(0)U^2}{2} + \frac{cg'(0)}{[g(0)]^2}UV - D'(0)V^2.$$

Following the technique of Andronov et al. (1972), we perform the change of variables:

$$\tilde{\tau} = -c\tau, \ \phi_1 = U, \ \phi_2 = \frac{f'(0)U}{c} + \frac{V}{g(0)}, \tag{22}$$

which, using the fact that $U' = -c\frac{\mathrm{d}\phi_1}{\mathrm{d}\tilde{\tau}}$ and $V = g(0)\left(\phi_2 - \frac{f'(0)\phi_1}{c}\right)$, transforms (21) into the system:

$$\begin{cases} \phi_1' = -\frac{D'(0)g(0)}{c}\phi_1\left(\phi_2 - \frac{f'(0)\phi_1}{c}\right) := \bar{F}_2(\phi_1,\phi_2), \\ \phi_2' = \phi_2 + \bar{G}_2(\phi_1,\phi_2), \end{cases} \tag{23}$$

where

$$\bar{G}_2(\phi_1,\phi_2) := \left(\frac{f''(0)}{2c} + \frac{g'(0)f'(0)}{cg(0)} + \frac{D'(0)[g(0)f'(0)]^2}{c^3}\right)\phi_1^2 - \left(\frac{2D'(0)f'(0)g^2(0)}{c^2} + \frac{g'(0)}{g(0)}\right)\phi_1\phi_2 + \frac{D'(0)g^2(0)}{c}\phi_2^2.$$

Let $\varphi(\phi_1)$ be the solution to $\phi_2 + \bar{G}_2(\phi_1,\phi_2) = 0$, i.e., $\varphi(\phi_1) = -\bar{G}_2(\phi_1,\varphi(\phi_1))$. For notational simplicity let

$$A := \frac{f''(0)}{2c} + \frac{g'(0)f'(0)}{cg(0)} + \frac{D'(0)[g(0)f'(0)]^2}{c^3},$$
$$B := -\left(\frac{2D'(0)f'(0)g^2(0)}{c^2} - \frac{g'(0)}{g(0)}\right),$$

and

$$E := \frac{D'(0)g^2(0)}{c},$$

and define $\mathcal{F} : \mathbb{R}^2 \to \mathbb{R}$ as

$$\mathcal{F}(\phi_1,\phi_2) = E\phi_2^2 + (B\phi_1 + 1)\phi_2 + A\phi_1^2.$$

Observe that $\mathcal{F}$ satisfies: $\mathcal{F}(0,0) = 0$, $\mathcal{F}_{\phi_1}, \mathcal{F}_{\phi_2}$ are continuous for all ϕ_1, ϕ_2, and $\frac{\partial \mathcal{F}}{\partial \phi_2}(0,0) = 1$. Hence, the Implicit Function Theorem gives the existence of a neighborhood $V_\delta(0,0)$ about $(0,0)$ such that $\mathcal{F}(\phi_1,\phi_2) = 0$. This provides a unique solution $(\phi_1, \varphi) : V_\delta(0,0) \to \mathbb{R}$ such that:

1. $\mathcal{F}(\phi_1, \varphi(\phi_1)) = 0$,
2. $\varphi'(\phi_1) = \frac{\mathcal{F}_{\phi_1}}{\mathcal{F}_{\phi_2}}$.
3. $\varphi(0) = \varphi'(0) = 0$.

In fact, from the definition of $\mathcal{F}$ we see that:

$$\varphi(\phi_1) = \frac{1}{2E}\left[-(B\phi_1 + 1) + \sqrt{(B\phi_1+1)^2 - 4AE\phi_1^2}\right]. \tag{24}$$

Hence, $\varphi(0) = 0$ and it can also be verified that $\varphi'(0) = 0$. Now, let

$$\Phi(\varphi(\phi_1)) = \bar{F}_2(\phi_1,\varphi(\phi_1)) = -\frac{E}{g(0)}\phi_1\left(\varphi(\phi_1) - \frac{f'(0)\phi_1}{c}\right).$$

Note that $\Phi(0) = \Phi'(0) = 0$ and $\Phi''(0) = -2Ef'(0)/(g(0)c) \neq 0$ given assumption (M). Thus, an application of Theorem 6 (found in "Appendix B") gives that the point

P_0 is a *saddle-node* of system (23). Moreover, since (22) defines a linear transformation between the UV-plane and $\phi_1\phi_2$-plane we see that P_0 is also a *saddle-node* for system (21). Now, by the Center Manifold Theorem (Theorem 3) we observe that (21) has a unique stable one-dimensional invariant manifold that is locally tangent to the eigenvector $(0, 1)^{\mathrm{T}}$ as well as a invariant center manifold which is locally tangent to the eigenvector $(c/g(0), -f'(0))^{\mathrm{T}}$. All trajectories close to P_0, with the exception of the trajectory on the stable manifold, will converge to the center manifold, and so it suffices to understand the center manifold dynamics near P_0. For this purpose, note that the equation for the center manifold near P_0 takes the form:

$$[M\varphi](\phi_1)=\varphi'(\phi_1)D'(0)\varphi\phi_1+f'(0)\phi_1+\frac{c\varphi}{g(0)}+\frac{f''(0)\phi_1^2}{2}+\frac{cg'(0)}{[g(0)]^2}\phi_1\varphi+D'(0)\varphi^2.$$

Refer to "Appendix A" for more details. Note that if $\varphi(\phi_1) = O(\phi_1^k)$ for $k > 1$ then the above equation becomes:

$$[M\varphi](\phi_1) = f'(0)\phi_1 + \frac{c\varphi}{g(0)} + \frac{f''(0)\phi_1^2}{2} + \frac{cg'(0)}{[g(0)]^2}\phi_1\varphi + O(\phi_1^{2k}).$$

Hence, if

$$\varphi(\phi_1) = -\frac{[g(0)]^2\left(f'(0) + \frac{f''(0)\phi_1}{2}\right)\phi_1}{c[g(0) + g'(0)\phi_1]} \tag{25}$$

then $[M\varphi](\phi_1) = O(\phi_1^{2k})$. Then, an application of Theorem 5 (see "Appendix A") yields that (25) provides a good approximation of φ. Furthermore, the flow on the center manifold (denoted by $W^C(P_0)$) can be approximated by:

$$\begin{aligned}\phi_1' &= F_1(\phi_1, \varphi(\phi_1)) \\ &\approx -\frac{D'(0)g^2(0)}{c}\phi_1^2\left[\frac{f'(0) + \frac{f''(0)\phi_1}{2}}{g(0) + g'(0)\phi_1}\right].\end{aligned} \tag{26}$$

From Fig. 4 we observe that for $\phi_1 \neq 0$ and small $\phi_1' < 0$. Hence, the trajectories tend to P_0 along the center manifold for $\phi_1 > 0$ and away from P_0 for $\phi_1 < 0$. This implies that the nodal sector of P_0 lies on the positive ϕ_1 plane and the saddle point of the sector lies on the negative ϕ_1 side of the plane. We confirm this numerically in Fig. 5a for functions:

$$\beta(u) = u,\ g(u) = \frac{1}{1+u},\ f(u) = u(1-u),\ c = 1. \tag{27}$$

We conclude the local analysis by studying the equilibrium point $P_1 = (1, 0)$. Here, we see that the Jacobian is given by:

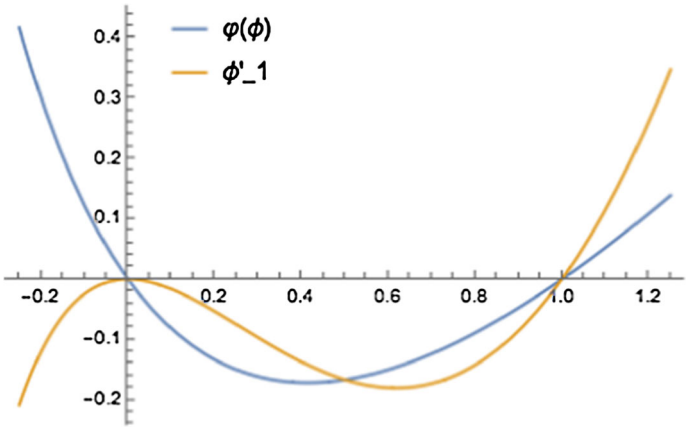

Fig. 4 (Color figure online) Plot of $\varphi(\phi_1)$ given in (25) and of the flow ϕ_1' on $W^C(P_0)$ given in (26)

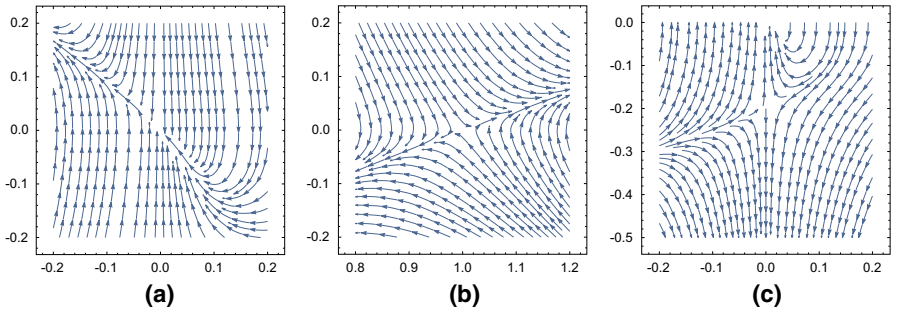

Fig. 5 (Color figure online) Local phase plane for (18) with rate functions given in (27). **a** illustrates the local phase plane about the point P_0, **b** illustrates the local phase plane about the point P_1, and **c** illustrates the local phase plane about the point P_c. **a** P_0. **b** P_1. **c** P_c

$$J[F,G]_{(1,0)} = \begin{bmatrix} 0 & D(1) \\ -f'(1) & -\frac{c}{g(1)} \end{bmatrix}.$$

Hence, the eigenvalues are given by:

$$\lambda_{\pm} = \frac{1}{2}\left\{ -\frac{c}{g(1)} \pm \sqrt{\left(\frac{c}{g(1)}\right)^2 - 4D(1)f'(1)} \right\}.$$

Under the condition that $f'(1) < 0$ then we have a saddle point, with $\lambda_+ > 0$ and $\lambda_- < 0$ with eigenvectors $(D(1), \lambda_+)^{\mathrm{T}}$ and $(D(1), \lambda_-)^{\mathrm{T}}$, respectively. This is confirmed in Fig. 5b. Finally, the point $P_2 := \left(0, -\frac{c}{g(0)D'(0)}\right) = (0, v_c)$ has Jacobian

$$J[F,G]_{(0,v_c)} = \begin{bmatrix} -\frac{c}{g(0)} & 0 \\ -\frac{c^2 g'(0)}{[g(0)]^3 D'(0)} - f'(0) - \frac{D''(0)c^2}{[D'(0)g(0)]^2} & \frac{c}{g(0)} \end{bmatrix}.$$

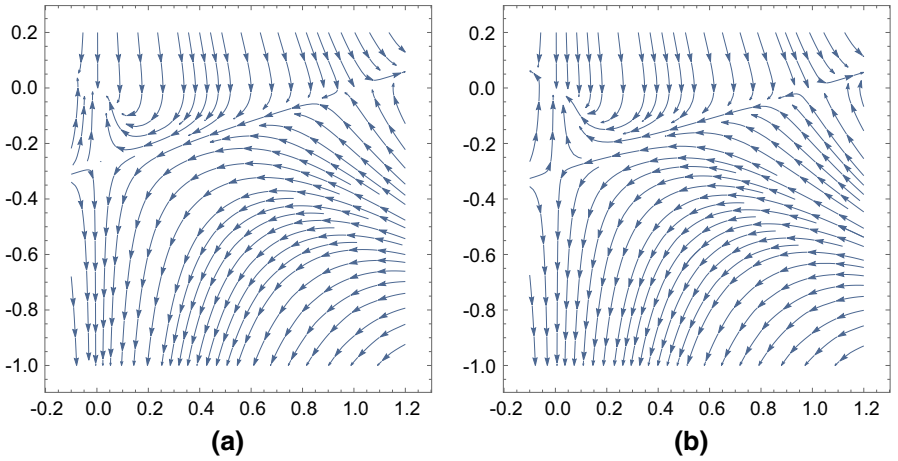

Fig. 6 (Color figure online) Global phase plane for (18) with rate functions given in (27). **a** illustrates the case when $c = 1.4$ and **b** when $c = 1.5$.

This matrix has eigenvalues: $\lambda_{\pm} = \pm\frac{c}{g(0)}$ and so it is a saddle point. The unstable eigenvalue is given by $(0, 1)^{\mathrm{T}}$ and the stable eigenvalue by $(1, l)^{\mathrm{T}}$ with $l = \left(\frac{c^2 g'(0)}{[g(0)]^3 D'(0)} + f'(0) + \frac{D''(0)c^2}{[D'(0)g(0)]^2}\right)\frac{g(0)}{2c}$ (Fig. 6).

Case 2: Degenerate bistable case $f'(0) = 0,\ f''(0) > 0$. Much of the analysis for this case is the same as for the monostable case so we omit most details and only point out the differences. Here, a similar change of variables removes the singularity and the Jacobian is given by (19). For the point P_0 the eigenvalues remain as $\lambda_1 = 0$ and $\lambda_2 = -\frac{c}{g(0)} < 0$, with eigenvectors $(1, 0)^{\mathrm{T}}$ and $(0, 1)^{\mathrm{T}}$, respectively. Once again P_0 is a non-hyperbolic equilibrium and we must look at a second-order approximation. The remaining analysis is similar, but system (23) now reads as:

$$\begin{cases} \phi_1' = -\frac{D'(0)g(0)}{c}\phi_1\phi_2 := \bar{F}_2(\phi_1, \phi_2), \\ \phi_2' = \phi_2 + \bar{G}_2(\phi_1, \phi_2), \end{cases} \tag{28}$$

now with $\bar{G}_2(\phi_1, \phi_2) := \frac{f''(0)}{2c}\phi_1^2 - \frac{g'(0)}{g(0)}\phi_1\phi_2 + \frac{D'(0)g^2(0)}{c}\phi_2^2$. Now, the solution to $\phi_2 + \bar{G}_2(\phi_1, \phi_2)) = 0$ is still given by (24) with:

$$A := \frac{f''(0)}{2c},\ B := -\frac{g'(0)}{g(0)},\ E := \frac{D'(0)g^2(0)}{c}.$$

Direct computations show that $\varphi(0) = \varphi'(0) = 0$ and $\varphi''(0) = -f''(0)/c$. Moreover, observe that now

$$\Phi(\varphi(\phi_1)) = -\frac{E}{g(0)}\phi_1\varphi(\phi_1),$$

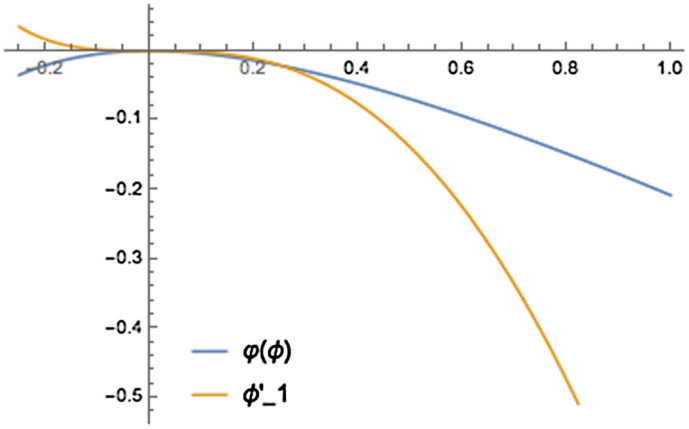

Fig. 7 (Color figure online) Plot of $\varphi(\phi_1)$ given in (25) and of the flow ϕ_1' on $W^C(P_0)$ given in (30)

from which we can compute that $\Phi(\varphi(0)) = \Phi'(\varphi(0)) = \Phi''(\varphi(0)) = 0$ and

$$\Phi'''(\varphi(0)) = -3\frac{E}{g(0)}\varphi''(0) = \frac{D'(0)g(0)f''(0)}{c^2}.$$

Hence, invoking Theorem 6 now gives that P_0 is a topological node.

Preforming a similar analysis to approximate $\varphi(\phi_1)$ and the flow on $W^C(P_0)$ we see that (25) is replaced by:

$$\varphi(\phi_1) = -\frac{[g(0)]^2 f''(0)\phi_1^2}{2c[g(0) + g'(0)\phi_1]} \tag{29}$$

and the flow is now given by:

$$\phi_1' = -\frac{D'(0)g^2(0)f''(0)\phi_1^3}{2c(g(0) + g'(0)\phi_1)} + o(\phi_1^{2k+1}). \tag{30}$$

See Fig. 7. These results are confirmed numerically in Fig. 8.

4.3 Preliminary Results: Monostable Case

In this subsection, we state and prove some preliminary results, such as monotonicity, uniqueness of sharp waves, and nonexistence. First, let us define some useful notation. Let $W_c^U(P)$ be the C^r-unstable manifold ($r \geq 2$) which is tangent to the unstable subspace of the equilibrium point P and $W_c^s(P)$ be the C^r-stable manifold which is tangent to the stable subspace of the equilibrium point P. Also, let $V_c(U)$ denote the path of $W_c^s(P_c)$. For a fixed speed $c > 0$ let the $W_c^s(P_c)$-**exit point** be the exit point of the path of $W_c^s(P_c)$ (backwards in time) of the set

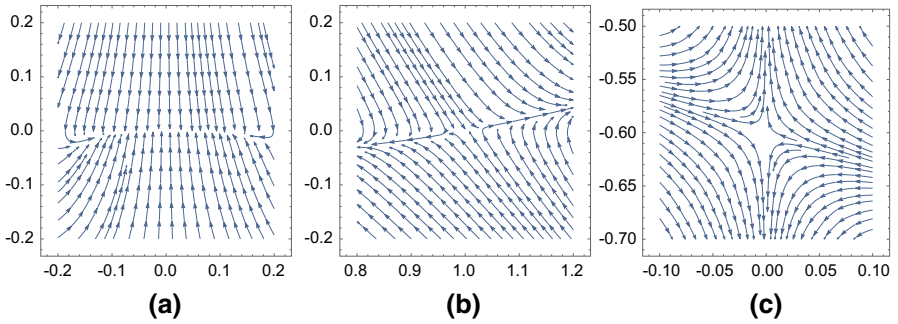

Fig. 8 (Color figure online) Local phase plane for (18) with rate functions given in (13) and (14) with $\mu = 1, \bar{m}u = .5,\ c = 1.2$. Figure 5a illustrates the local phase plane about the point P_0, 5b illustrates the local phase plane about the point P_1, and 5c illustrates the local phase plane about the point P_c. **a** P_0. **b** P_1. **c** P_c

$$\{(U, V) : 0 \leq U \leq 1, V < 0\},$$

and we denote it by (U_c, V_c). Finally, we define

$$c^* = \inf\{c > 0 : U_c = 1, v_c < 0\}. \tag{31}$$

From (18) we see that

$$\frac{\mathrm{d}V}{\mathrm{d}U} = -\frac{cV + g(U)f(U) + D'(U)g(U)V^2}{g(U)D(U)V}.$$

Let $V_1(U)$ and $V_2(U)$ be solution trajectories such that $V_1(1) = V_2(1) = 0$ corresponding to speeds c_1 and c_2, respectively. We obtain the following monotonicity result:

Lemma 1 (Monotonicity) *Let $V_1(U)$ and $V_2(U)$ be solution trajectories such that $V_1(1) = V_2(1) = 0$ corresponding to speeds c_1 and c_2, respectively. Additionally, assume that $V_1(U)V_2(U) > 0$ for all $U \in (0, 1)$. Then, the following holds:*

(i) *If $c_1 = c_2$ then $V_1(U) = V_2(U)$ for $U \in (0, 1)$;*
(ii) *If $c_1 > c_2$ then $V_1(U) > V_2(U)$ for $U \in (0, 1)$.*

Proof Define $w(U) = V_2(U) - V_1(U)$ and note that $w(1) = 0$ and satisfies:

$$w' = \frac{c_1 - c_2}{g(U)D(U)} + Q(U)w,$$

with

$$\begin{aligned} Q(U) &= \frac{f(U)g(U)(V_2 - V_1) + D'(U)g(U)(V_1^2V_2 - V_2^2V_1)}{D(U)g(U)V_1V_2(V_2 - V_1)} \\ &= \frac{f(U)g(U)}{D(U)V_1V_2} - \frac{D'(U)}{D(U)}. \end{aligned}$$

Equivalently, in integral form we obtain:

$$w(U) = w(1)\exp\left\{-\int_U^1 Q(s)\,\mathrm{d}s\right\} - (c_1 - c_2)\int_U^1 \frac{1}{D(\tilde{U})g(\tilde{U})}\exp\left\{\int_{\tilde{U}}^1 Q(s)\,\mathrm{d}s - \int_U^1 Q(s)\,\mathrm{d}s\right\}\,\mathrm{d}\tilde{U}, \tag{32}$$

for $U \in (0, 1)$. We now verify that the integrals in (32) are bounded. Indeed, we have that

$$\int_U^1 Q(s)\,\mathrm{d}s = \int_U^1 \frac{f(s)g(s)}{D(s)V_1(s)V_2(s)}\,\mathrm{d}s + \ln(D(U)) - \ln(D(1)).$$

Note that under the assumption that $V_1(s)V_2(s) > 0$ for all $s \in (0, 1)$ we see that the integral on the RHS of the above equation is always positive. Noting that $\ln(D(U)) > -\infty$ for $U \in (0, 1]$ we conclude that the RHS of (32) is well-defined. Now, taking into account that $w(1) = 0$ we see that if $c_1 = c_2$ when $w(U) \equiv 0$ for $U \in (0, 1)$ implying that (i) holds. However, if $c_1 > c_2$ then we see that $w(U) < 0$ implying that (ii) holds. □

Almost immediately, as a consequence of Lemma 1 we obtain a uniqueness result for the traveling wave solution of sharp-type.

Proposition 2 (Uniqueness of sharp-type traveling wave solution) *If there exists a traveling wave solution satisfying* (15) *with then travels with a unique speed* $c^* > 0$.

Proof Assume for contradiction that there exist two such waves U_1 and U_2 with speed c_1^* and the other with c_2^*, respectively. Without loss of generality assume that $c_1^* > c_2^*$. Then, we know that

$$U_1'(z^{*-}) = -\frac{c_1^*}{g(0)D'(0)} \quad \text{and} \quad U_2'(z^{*-}) = -\frac{c_2^*}{g(0)D'(0)}.$$

This implies that $V_1(0) < V_2(0)$ and by continuity there exists some $U > 0$ such that $V_1(U) < V_2(U)$ due to the local analysis of P_c. This contradicts Lemma 1, and we conclude. □

4.3.1 Nonexistence Result

In this section, we prove the nonexistence of traveling wave solutions as given in Definition 2 or continuously differentiable traveling wave solutions as in Definition 1. First, consider the case when $c = 0$ then the ODE in non-degenerate coordinates (18) becomes:

$$\begin{cases} U' = D(U)V, \\ V' = -D'(U)V^2 - f(U). \end{cases} \tag{33}$$

We compare the trajectories of (33) to those of the system:

$$\begin{cases} U' = [D(U)]^2 V, \\ V' = -D'(U)D(U)V^2 - f(U)D(U). \end{cases} \tag{34}$$

Given that $D(U) > 0$ for $U \in (0, 1]$ and C^r with $r \geq 2$, then the paths of the trajectories of systems (33) and (34) coincide in the region:

$$\mathcal{S} := \{(U, V) : 0 < U \leq 1, -\infty < V < \infty\}.$$

The benefit of working with (34) is that it has a Hamiltonian given by:

$$H(U, V) = \frac{1}{2}[D(U)V]^2 + \int_{U_0}^{U} D(s)f(s)\, \mathrm{d}s.$$

Indeed, we have that

$$\begin{cases} U' = \frac{\partial H}{\partial V}, \\ V' = -\frac{\partial H}{\partial U}. \end{cases}$$

So the trajectories of (34) are those given by the level-set curves of $H(U, V) = C$.

Lemma 2 *For $c \geq 0$ sufficiently close to zero the trajectory $V(U)$ leaving P_1 (on $W_c^U(P_1)$) is such that*

$$\lim_{U \to 0^+} V(U) = -\infty.$$

Moreover, for $c > 0$ (and sufficiently small) the trajectory on $W_c^s(P_c)$ leaves the region

$$\mathcal{S} := \{(U, V) : 0 < U \leq 1, -\infty < V < 0\},$$

backwards in time, at some point U_0 with $U_0 \in (0, 1)$.

Proof First, consider the case $c = 0$. Here, the trajectory passing through the point $(1, 0)$ must satisfy:

$$\frac{1}{2}[D(U)V]^2 + \int_{U_0}^{U} D(s)f(s)\, \mathrm{d}s = H(1, 0) = \int_{U_0}^{1} D(s)f(s)\, \mathrm{d}s.$$

Then, solving directly for V yields:

$$V(U) = \pm \frac{1}{D(U)} \sqrt{2\left(\int_{U_0}^{1} D(s)f(s)\, ds - \int_{U_0}^{U} D(s)f(s)\, \mathrm{d}s\right)}.$$

For our boundary conditions we consider values on the negative branch. Note that under our conditions on D and f we have that

$$\int_{U_0}^{U} D(s) f(s)\, \mathrm{d}s,$$

is strictly positive, increasing on (0,1], and attain a maximum at $U = 1$. Thus, $V \to -\infty$ as $U \to 0^+$ and by continuity this is true for small values of c as well. With this we conclude the first part of the lemma. For the second part, note that the trajectories on $W_c^u(P_1)$ and $W_c^s(P_c)$ cannot cross by uniqueness of the ode system. Hence, $W_c^s(P_c)$ must exit $\mathcal{S}$ in reverse time through some point $U_0 \in (0, 1)$. □

4.3.2 Existence of Monotone Waves for Large Speeds c

We now prove the existence of continuously differentiable traveling fronts for large speeds. For this purpose, we define

$$M := \max_{s\in(0,1)} 4D'(u) f(u) g^2(u). \tag{35}$$

Note that M is well-defined since D', f and g are bounded on the interval [0, 1]. They are also strictly positive inside the interval (0, 1) with $D'(u) f(u) g^2(u) = 0$ when $u \in \{0, 1\}$. Hence, we know that the maximum of M is achieved for at most a finite number of points $\{u_1, u_2, \ldots, u_n\}$ for some $n \in \mathbb{N}$.

Proposition 3 (Existence of continuously differentiable traveling wave solution) *Let the conditions of Theorem 2 hold and $c \geq \sqrt{M}$ with M defined in (35). Then, there exists smooth traveling wave solutions (in the sense of Definition 1), which are solution to (6).*

Proof We prove that for speeds $c \geq \sqrt{M}$ there are traveling wave solutions connecting the points P_1 and P_0. This ODE-type proof relies on finding a region that traps the trajectory coming out of the unstable direction of P_1. For this purpose, consider the nullclines of U and V. Note that $U' = 0$ when $U = 0$ or $V = 0$. Moreover, for $V < 0$ and $U \in (0, 1]$ it holds that $U' < 0$. On the other hand, the V-nullclines are given by:

$$V_{\pm}(U) = \frac{-c \pm \sqrt{c^2 - 4D'(U) f(U) g^2(U)}}{2D'(U) g(U)}. \tag{36}$$

From (36) we observe that $V_-(U) \leq V_+(U) \leq 0$ for all $U \in [0, 1]$, $V_+(0) = V_+(1) = 0$ and

$$V_-(0) = -\frac{c}{D'(0) g(0)} \quad \text{and} \quad V_-(1) = -\frac{c}{D'(1) g(1)}.$$

Case 1: ($c > \sqrt{M}$) In this case it always holds that $V_-(U) < V_+(U) \leq 0$ on [0, 1] so there exists a $\phi_2 \in (V_-(U), V_+(U))$ for all $U \in [0, 1]$. Now, consider the rectangle R with the following boundaries:

$$\ell_1 := \{U = 1, \phi_2 \le V \le 0\}, \ell_2 := \{U = 0, \phi_2 \le V \le 0\},$$
$$\ell_3 := \{0 \le U \le 1, V = 0\}, \ell_4 := \{0 \le U \le 1, V = \phi_2\}.$$

Step 1: We prove that R is an invariant set: any trajectory that starts on that rectangle is trapped there. To see this, note that on ℓ_1 we have that $U' \le 0$ and $V' \ge 0$. On ℓ_2 we have that $U' = 0$ and $V' > 0$, on ℓ_3 we have that $U' = 0$ and $V' < 0$, and on ℓ_4 we have that $U' < 0$ and $V' > 0$. Hence, on the boundaries all trajectories point into R.
Step 2: Next, we show that the trajectory coming out of P_1 in the unstable direction lies within R. To see this, recall that the slope of the trajectory at P_1 is given by:

$$\lambda_+ = \frac{1}{2}\left\{-\frac{c}{g(1)} + \sqrt{\left(\frac{c}{g(1)}\right)^2 - 4D(1)f'(1)}\right\}, \tag{37}$$

which is greater than zero as $f'(1) < 0$. Since the only other equilibrium point is P_0 the trajectory must end there. Thus, we have a heteroclinic trajectory connecting P_0 and P_1. Note that this immediately proves the monotonicity of the traveling wave. □

Case 2: ($c = \sqrt{M}$) In this case, we have that there are possibly a finite number of points $\{u_1, u_2, \ldots, u_n\}$ where M is achieved and so $V_+(u_i) = V_-(u_i)$ for $i = 1, 2, \ldots, n$. Also, a direct computation shows that $V'_+(1) = -\frac{f'(1)g(1)}{c}$ and since the trajectory coming out of P_1 in the unstable direction has slope given by (37) we know that this trajectory starts out in the region $R_1 := \{0 \le U \le 1, V_+(U) < V < 0\}$. In this region, the trajectory is pushed toward $V_+(U)$ and if it exists the region at a point U_0 such that $U_0 > u_i$ for any $i \in \{1, 2, \ldots n\}$ then it will immediately be pushed by into R_1. On the other hand, if it exists at U_0 such that $U_0 < u_i$ for all $i \in \{1, 2, \ldots, n\}$ then the flow pushes the trajectory toward P_0.

In either case, we have established the existence of a heteroclinic orbit connecting P_0 to P_1. This provides the monotone traveling wave solution which we seek.

4.3.3 Existence of a Sharp Wave for c^*

In this subsection, we state some lemmas that will be useful in proving the existence of a sharp wave.

Lemma 3 (Monotonicity of V_c) *Let $c_1 < c_2$ then $V_{c_1}(U) > V_{c_2}(U)$ for $U \in [0, 1]$.*

Proof Note that for $c_1 < c_2$ then $V_{c_1}(0) > V_{c_2}(0)$ since $V_c(0) = -c/D'(0)g(0)$. Then, by continuity it holds that $V_{c_1}(U) > V_{c_2}(U)$ for $U \in (0, U^*)$ for some $U \ge 0$. Now, assume for contradiction that $U^* \le 1$ and define

$$w(U) = V_{c_1}(U) - V_{c_2}(U).$$

Note that $w(U^*) = 0$ and, following the steps of the proof of Lemma 1, we obtain that for $U \in (0, U^*)$

$$w(U) = w(U^*) \exp\left\{-\int_U^{U^*} Q(s)\, \mathrm{d}s\right\} - (c_1 - c_2) \int_U^{U^*} \frac{1}{D(\tilde{U})g(\tilde{U})} \exp\left\{-\int_{\tilde{U}}^{U^*} Q(s)\, \mathrm{d}s\right\} \mathrm{d}\tilde{U}. \quad (38)$$

One can similarly prove that the integrals are bounded. Then, since $w(U^*) = 0$ and the integrals are positive we conclude that $w(U) > 0$, which gives us a contradiction. □

Lemma 4 *The critical speed c^* defined in (31) is well-defined and $V_{c^*} = 0$.*

Proof Lemma 2 tells us that for c positive but close to zero it holds that $0 < U_c < 1$ and $V_c = 0$. Hence, c^* has a lower bound. For an upper bound note that for $c > \sqrt{M}$ it holds that $U_c = 1$ and $V_c < 0$. This is due to the fact that the invariance of the rectangle R defined in the proof of Proposition 3 (*case 1*) prevents the exit point to be such that $0 < U_c < 1$ and $V_c > \phi_2$ (with ϕ_2 defined in the proof of Proposition 3. Hence, $0 < c^* < \sqrt{M}$. Now, by continuity of the solution trajectories with respect to c as well as the monotonicity provided in Lemma 3 gives that $V_{c^*} = 0$. □

4.4 Proof of Main Result

We are now ready to prove Theorem 2.

Proof To see that (i) holds we simply note that for any $c < c^*$ continuity gives that the $W_c^s(P_c)$-exit point satisfies $0 < U_c < 1$ and $V_c(U_c) = 0$. Hence, there cannot be any heteroclinic connections between the points P_0 and P_1 (else the two trajectories must cross contradicting uniqueness of the ODE system defined by (18)).

To prove (iii) note that for $c > c^*$ it holds that $V_c < 0$ and $U_c = 1$. From this we can obtain an invariant region with the $W_c^s(P_c)$ trajectory providing a boundary. Then, the trajectory leaving P_1 in the unstable direction must approach P_0.

Finally, to prove (ii) we show by contradiction that $U_{c^*} = 1$ and $V_{c^*} = 0$. If this is not the case then either (*a*) $U_{c^*} = 1$ and $V_{c^*} < 0$ or (*b*) $U_{c^*} < 1$ and $V_{c^*} = 0$. Now, by Lemma 4 we know that (*a*) cannot occur. Assuming (*b*) occurs then take c larger but close to c^*. Then, by Lemma 3 we have that $V_c(U) < V_{c^*}(U) \leq 0$ and $0 < U_{c^*} < U_c < 1$; hence, c violates the definition of c^*. Uniqueness follows by Proposition 2. □

5 Discussion

The potential existence of sharp traveling waves and their related stability conditions have implications for expectations of responses to climate change. Sharp and stable traveling waves imply a solid front to an advance of a species or a type of vegetation

into new area. This type of boundary is observed for some ecotones (Harsch and Bader 2011) but is usually attributed to an underlying environmental discontinuity (Butler et al. 2008) or to a positive feedback switch that creates such a discontinuity (Wilson and Agnew 1992). The results here indicate another process through which the rate of climate change and the rate of an ecological response could be decoupled.

In Malanson and Rodríguez (2017), working in parallel on the ABM was able to develop sharp traveling waves only in a limited (and probably ecologically unrealistic) context. The dialectic with this work here, however, enables further examination of the details of traveling waves. These may go beyond demonstrating their existence to consideration of feedbacks between their shapes and the processes that create them.

Acknowledgements The authors are grateful to Thomas Hillen for interesting discussions. Nancy Rodríguez was partially supported by NSF DMS-1516778.

A Center Manifold Theorem

Let $n \geq 2$ and consider the system

$$x' = F(x),\ x \in \mathbb{R}^n,\ F : \mathbb{R}^2 \to \mathbb{R}^n, \tag{39}$$

with $F \in C^r(\mathbb{R}^2)$ for $r \geq 2$ and fixed point x_0, *i.e.,* that is $F(x_0) = 0$. Consider the linearized system of (39) about the

$$x' = Ax,$$

where A is a $n \times n$ matrix. Assume that A has n real and distinct eigenvalues $\{\lambda_1, \lambda_2, \ldots, \lambda_n\}$ with corresponding eigenvectors $\{v_1, v_2, \ldots, v_n\}$.

Definition 3 The set $E_s = span\{v_i : \lambda_i < 0\}$ is the *stable subspace* of the equilibrium x_0. The set $E_u = span\{v_i : \lambda_i > 0\}$ is the *unstable subspace* of the equilibrium x_0. The set $E_c = span\{v_i : \lambda_i = 0\}$ is the *center subspace* of the equilibrium x_0.

It is easily proved that $\mathbb{R}^n = E_s \oplus E_u \oplus E_c$. In the analysis to follow we will take advantage of the following theorem.

Theorem 3 (Center manifold theorem Bressan et al. 2003; Carr 1981) *Let $f \in C^r$ be a vector field on $\mathbb{R}^n$ which vanishes at the origin, i.e., $f(0) = 0$ and let $A = Df(0)$. Let the stable, center, and unstable invariant subspaces associated with be as in Definition 3. Then, there exist C^r stable and unstable manifolds W_s, W_u tangent to E_s, E_u, respectively, and a C^{r-1} center manifold W_c tangent to E_c. Moreover, the manifolds W_s, W_u, and W_c are invariant under the flow f.*

Consider the case when the unstable manifold of our system is empty and the system can be written in the form:

$$\begin{cases} x' = Ax + f(x, y) \\ y' = Bx + g(x, y), \end{cases} \tag{40}$$

with $x \in \mathbb{R}^p$ and $y \in \mathbb{R}^q$ with $p+q=n$ where A has eigenvalues with zero real part and B has eigenvalues with negative real part. The center manifold can be represented as

$$W^c = \{(x, y) : y = \varphi(x)\}, \ \varphi(0) = D\varphi(0) = 0, \ \varphi(x) : U \to \mathbb{R}^q,$$

with $U \subset \mathbb{R}^p$ containing the origin. A good approximation of the flow along W^c is then given by:

$$x' = Ax + f(x, \varphi(x)). \tag{41}$$

We will use the following reduction principle.

Theorem 4 (Reduction principle) *If the origin of* (4) *is asymptotically stable (unstable) then the origin of* (40) *is also asymptotically stable (unstable).*

In order to approximate $y = \varphi(x)$ we apply the chain rule on $\varphi(x)$ go back to the dynamics of (40). Indeed, we have

$$y' = D\varphi(x)x' = D\varphi(x)[Ax + f(x, \varphi)] = Bx + g(x, \varphi).$$

From this we obtain the expression on the manifold:

$$M[\varphi(x)] = D\varphi(x)[Ax + f(x, \varphi)] - Bx - g(x, \varphi) = 0, \quad \varphi(0) = D\varphi(0) = 0. \tag{42}$$

We use the following result to find a suitable approximation of $\varphi(x)$.

Theorem 5 (Approximation of $\varphi(x)$) *If a function $\tilde{\varphi}(x)$ with $\tilde{\varphi}(0) = \tilde{D}\varphi(0) = 0$ can be found such that $M[\tilde{\varphi}(x)] = O(|x|^m)$ for $m > 1$ as $|x| \to 0$ then it holds that*

$$\varphi(x) = \tilde{\varphi}(x) + O(|x|^m) \text{ as } |x| \to 0.$$

B Behavior About a Plane Non-Hyperbolic Point

In this section, we discuss the theory developed by Andronov et al. in Andronov et al. (1972) for the behavior of a point that is non-hyperbolic. For this purpose, consider the 2×2 system

$$\begin{cases} x' = ax + by + f(x, y) \\ y' = cx + dy + g(x, y), \end{cases} \tag{43}$$

where f, g are analytic functions around the origin with zero a unique isolated fixed point. Moreover, assume that

$$a + d = 0 \quad \text{and} \quad ad - bc = 0.$$

When $a = b = 0$ (as is in our case) the change of variables $\tilde{x} = x$ and $\tilde{y} = (c/d)x + y$ changes (43) into a system of the form:

$$\begin{cases} \tilde{x}' = \tilde{f}(\tilde{x}, \tilde{y}) \\ \tilde{y}' = \tilde{y} + \tilde{g}(\tilde{x}, \tilde{y}), \end{cases} \tag{44}$$

with $\tilde{f}, \tilde{g}$ also analytic about the origin. First, we look for solutions to

$$\tilde{y} + \tilde{g}(\tilde{x}, \tilde{y}) = 0,$$

in a neighborhood of the origin. This solution $\varphi(\tilde{x})$ is obtained using the Implicit Function Theorem, which also guarantees that $\varphi(0) = \varphi'(0) = 0$. Next, note that

$$\Phi(\tilde{x}) := \tilde{f}(\tilde{x}, \varphi(\tilde{x})),$$

is not exactly zero since the origin is an isolated equilibrium. Hence, we expand $\Phi(\tilde{x})$:

$$\Phi(\tilde{x}) \approx K_m x^m + \cdots,$$

with $m \geq 2$ and $K_m \neq 0$. We will use the following theorem.

Theorem 6 (Andronov et al. 1972) *Let* $(0, 0)$ *be an isolated fixed point of* (44)*, and let* $\varphi(\tilde{x})$ *and* $\Phi(\tilde{x})$ *defined as above. Then:*

1. *If* m *is odd and* $K_m > 0$ *then the origin is a topological node.*
2. *If* m *is odd and* $K_m < 0$ *then the origin is a topological saddle point.*
3. *If* m *is even, then the origin is a saddle-node (it canonical neighborhood is the union of one parabolic and two hyperbolic sectors). If* $K_m < 0$*, the hyperbolic sector contains a segment of the positive* x*-axis bordering the origin and if* $K_m > 0$ *they contain a segment of the negative* x*-axis.*

References

Andronov AA, Leontovich EA, Gordon II, Maier AG (1972) Theory of dynamical systems on a plane. Israel Program for Scientific Translations, Jerusalem

Bates PW, Fife PC, Ren X, Wang X (1997) Traveling waves in a convolution model for phase transitions. Arch Ration Mech Anal 138:105–136

Betts RA, Cox PM, Collins M, Harris PP, Huntingford C, Jones CD (2004) The role of ecosystem-atmosphere interactions in simulated Amazonian precipitation decrease and forest dieback under global climate warming. Theoret Appl Climatol 78(1–3):157–175

Bressan A, Serre D, Williams M, Zumbrun K (2003) Tutorial on the center manifold theorem. In: Hyperbolic systems of balance laws. Springer, Berlin. www.math.psu.edu/bressan/PSPDF/cmanif.pdf

Britton NF (1986) Reaction–diffusion equations and their applications to biology. Academic Press, London

Butler DR, Malanson GP, Walsh SJ, Fagre DB (2008) Influences of geomorphology and geology on alpine treeline in the American West—more important than climatic influences? Phys Geogr 28(5):434–450

Cantrell R, Cosner C, Cantrall RS, Cosner C (2003) Spatial ecology via reaction–diffusion equations. Ecology of predator-prey interactions. Wiley, West Sussex

Carr J (1981) Applications of centre manifold theory. Springer, Berlin

Chen X (1997) Existence, uniqueness, and asymptotic stability of traveling waves in nonlocal evolution equations. Adv Differ Equ 2(1):125–160

Coville J (2007) Travelling fronts in asymmetric nonlocal reaction diffusion equations: the bistable and ignition cases. Prépublication du CMM, Hal-006962:1–43
Coville J, Dupaigne L (2007) On a non-local equation arising in population dynamics. Proc R Soc Edinb Sect A 137(4):727–755
Coville J, Davila J, Martínez S (2008) Nonlocal anisotropic dispersal with monostable nonlinearity. J Differ Equ 244(12):3080–3118
Dey CJ, Richardson E, McGeachy D, Iverson SA, Gilchrist HG, Semeniuk CAD (2017) Increasing nest predation will be insufficient to maintain polar bear body condition in the face of sea ice loss. Glob Change Biol 23(5):1821–1831
Ermentrout GB, McLeod JB (1993) Existence and uniqueness of travelling waves for a neural network. Proc R Soc Edinb 123A:461–478
Evers JHM, Fetecau RC, Ryzhik L (2015) Anisotropic interactions in a first-order aggregation model. Nonlinearity 28(8):2847–2871
Grimm K, Railsback FS (2005) Individual-based modeling and ecology. Princeton University Press, Princeton
Harsch MA, Bader MY (2011) Treeline form—a potential key to understanding treeline dynamics. Glob Ecol Biogeogr 20(4):582–596
Hillen T, Greese B, Martin J, de Vries G (2015) Birth-jump processes and application to forest fire spotting. J Biol Dyn 9(sup1):104–127
Horvitz CC, Koop AL, Erickson KD (2015) Time-invariant and stochastic disperser-structured matrix models: invasion rates of fleshy-fruited exotic shrubs. Discrete Contin Dyn Syst Ser B 20(6):1639–1662
Hutson V, Martinez S (2003) The evolution of dispersal. J Math Biol 47:483–517
Jalbert E, Eberl HJ (2014) Numerical computation of sharp travelling waves of a degenerate diffusion–reaction equation arising in biofilm modelling. Commun Nonlinear Sci Numer Simul 19(7):2181–2190
Kawasaki K, Mochizuki A, Matsushita M, Umeda T, Shigesada N (1997) Modeling spatio-temporal patterns generated by bacillus subtilis. J Theor Biol 188(2):177–185
Kot M, Medlock J, Reluga T, Brian WD (2004) Stochasticity, invasions, and branching random walks. Theor Popul Biol 66(3):175–184
Li W-T, Sun Y-J, Wang Z-C (2010) Entire solutions in the Fisher-KPP equation with nonlocal dispersal. Nonlinear Anal Real World Appl 11(4):2302–2313
Malanson GP, Rodríguez N (2017) Traveling waves and spatial patterns from dispersal on homogeneous and gradient habitats. Ecol Complex 33(1):57–65
Malanson GP, Walsh SJ (2015) Agent-based models: individuals interacting in space. Appl Geogr 56:95–98
Malanson GP, Resler LM, Bader MY, Holtmeier F-K, Butler DR, Weiss DJ, Daniels LD, Fagre DB (2011) Mountain treelines: a roadmap for research orientation. Arct Antarct Alp Res 43(2):167–177
Mansour MBA (2007) Traveling wave solutions of a reaction–diffusion model for bacterial growth. Physica A 383(2):466–472
Mohd MH, Murray R, Plank MJ, Godsoe W (2016) Effects of dispersal and stochasticity on the presence–absence of multiple species. Ecol Model 342:49–59
Murray JD (2004) Mathematical biology, interdisciplinary applied mathematics, vol 17. Springer, New York
Othmer HG, Dunbar SR, Alt W (1988) Models of dispersal in biological systems. J Math Biol 26(3):263–298
Parmesan C, Yohe G (2003) A globally coherent fingerprint of climate change impacts across natural systems. Nature 421(6918):37–42
Pielou EC (1977) Mathematical ecology. Wiley, New York
Redmond MD, Kelsey KC, Urza AK, Barger NN (2017) Interacting effects of climate and landscape physiography on piñon pine growth using an individual-based approach. Ecosphere 8(3):e01681
Ruckstuhl KE, Johnson EA, Miyanishi K (2008) Introduction. The boreal forest and global change. Philos Trans R Soc B Biol Sci 363(1501):2243–2247
Sánchez-Garduño F, Maini PK (1994) Existence and uniqueness of a sharp travelling wave in degenerate non-linear diffusion Fisher-KPP equations. J Math Biol 33(2):163–192
Sánchez-Garduño F, Maini PK (1995) Traveling wave phenomena in some degenerate reaction–diffusion equations 117:281–319
Satnoianu RA, Maini PK, Sanchez-Garduño F, Arimtage JP (2001) Travelling waves in a nonlinear degenerate diffusion model for bacterial pattern formation. Discrete Contin Dyn B 1(3):339–362
Schellnhuber HJ (2009) Tipping elements in the earth system. Proc Nat Acad Sci 106(49):20561–20563

Smith-McKenna EK, Malanson GP, Resler LM, Carstensen LW, Prisley SP, Tomback DF (2014) Cascading effects of feedbacks, disease, and climate change on alpine treeline dynamics. Environ Model Softw 62:85–96

Sun YJ, Li WT, Wang ZC (2011) Traveling waves for a nonlocal anisotropic dispersal equation with monostable nonlinearity. Nonlinear Anal Theory Methods Appl 74(3):814–826

Travis JMJ, Delgado M, Bocedi G, Baguette M, Bartoń K, Bonte D, Boulangeat I, Hodgson JA, Kubisch A, Penteriani V, Saastamoinen M, Stevens VM, Bullock JM (2013) Dispersal and species' responses to climate change. Oikos 122(11):1532–1540

von Brecht JH, Uminsky DT (2017) Anisotropic assembly and pattern formation. Nonlinearity 30(1):225–273

Wilson JB, Agnew ADQ (1992) Positive-feedback switches in plant communities. Adv Ecol Res 23:263–336

Yagisita H (2009) Existence and nonexistence of traveling waves for a nonlocal monostable equation. Publ Res Inst Math Sci 45(4):925–953

Zeng Y, Malanson GP (2006) Endogenous fractal dynamics at alpine treeline ecotones. Geogr Anal 38:271–287